# An Optically Controlled MMW Beam-Steering Antenna Based on a Novel Architecture

V. A. Manasson, *Associate Member, IEEE*, L. S. Sadovnik, *Associate Member, IEEE*, V. A. Yepishin, *Associate Member, IEEE*, and D. Marker

***Abstract*— Beam-steering millimeter-wave (MMW) antennas using photo-induced plasma gratings (PIPG's) offer a dramatic decrease in fabrication cost compared to their phased-array counterparts. We describe a totally new antenna design which has been tested in both the receiving and the transmitting modes. The new antenna is a compact device with a reconfigurable PIPG in a semiconductor plate as an output aperture. This aperture is fed by a tunnel-coupling dielectric waveguide. We demonstrated the antenna's scanning capability over a $\pm$ 15° range. The new design permits the antenna to operate at various polarizations including linear polarization (either vertical or horizontal) and circular polarization (an ellipticity of only 0.8 dB has been demonstrated).**

***Index Terms*—Optical control, scanning MMW antennas.**

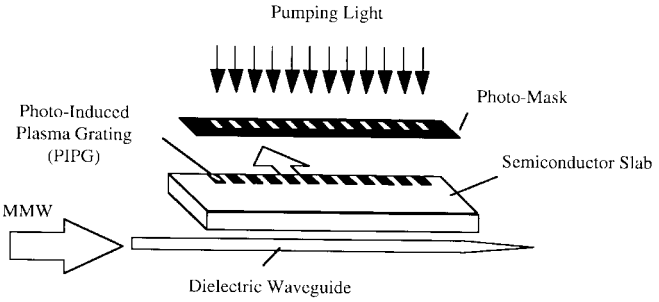


Fig. 1. Experimental setup.

## I. Introduction

DESPITE an enormous effort made to lower the cost of scanning phased-array antennas, the desired progress has yet to be achieved. However, as demonstrated recently, a photo-induced plasma excited in a semiconductor medium so as to form a periodic structure is a promising solution to inexpensive beam steering in the millimeter-wave (MMW) band [1]–[7]; in particular, for such price-sensitive applications as automobile-collision warning systems.

Several antenna designs utilizing this approach have been fabricated and tested. In most of them, the MMW signal propagates along a semiconductor waveguide or in a compound dielectric waveguide containing a photosensitive layer [1]–[4], [6]. By specially patterned illumination, a photo-induced plasma grating (PIPG) is excited on the surface of the waveguide. As in a leaky-wave antenna loaded with a metal grating [8], in an optically controlled antenna the MMW signal propagating along the semiconductor waveguide interacts with the plasma grating and couples out in a specific direction (at an angle $\varphi$) which depends on the grating period $\Lambda$. The main disadvantage of this design is that the PIPG also significantly attenuates the beam and prevents the MMW signal from effectively propagating along the waveguide. As a result, it becomes difficult to produce a radiating aperture of a reasonable size. In this paper, we present a new photonically controlled antenna architecture free of the above-mentioned shortcoming.

Manuscript received December 26, 1996; revised April 30, 1997. This work was supported by the Naval Surface Warfare Center under Contract N00178-96-C-003.

V. A. Manasson, L. S. Sadovnik, and V. A. Yepishin are with WaveBand Corporation, Torrance, CA 90501 USA.

D. Marker is with the Program Executive Office Theater Air Defense, Arlington, VA 22448-5100 USA.

Publisher Item Identifier S 0018-9480(97)06016-X.

## II. Antenna Design and Operation Principles

The new optically controlled antenna architecture is shown schematically in Fig. 1. The antenna consists of a semiconductor, a dielectric waveguide, and an illumination system. The semiconductor slab is cut from high-resistivity silicon. The dielectric waveguide is a quartz rod. The illumination system consists of a pulsed pumping light source and a set of photo-masks with different grating patterns. The pumping light illuminates the slab through one of the photo-masks, creating a plasma grating of the same configuration as the pattern on the mask.

The semiconductor slab represents a planar waveguide for the MMW's and is the main component of the antenna. The dielectric waveguide acts as a feeder, coupling the MMW into the semiconductor slab. The geometry of the MMW rays propagating through the slab is shown in Fig. 2. The propagation constant in the waveguide is smaller than that in the semiconductor slab $\beta_{\mathrm{wg}} < \beta_{\mathrm{sl}}$. The original Beam $\mathbf{A}$ propagates along the dielectric waveguide and tunnels into the semiconductor slab through the narrow gap between them. The small angle $\varepsilon$ ($\varepsilon < 3°$) between the slab edge (the lower facet in Fig. 2) and the waveguide was introduced to make the coupled Beam $\mathbf{B}$, more uniform along the $y$-direction. The Beam $\mathbf{B}$ width depends on the gap between the semiconductor slab and the quartz rod and can be set in a wide range. The propagation angle $\gamma$ inside the slab depends on the relation between the two propagation constants $\beta_{\mathrm{wg}}$ and $\beta_{\mathrm{sl}}$, and on

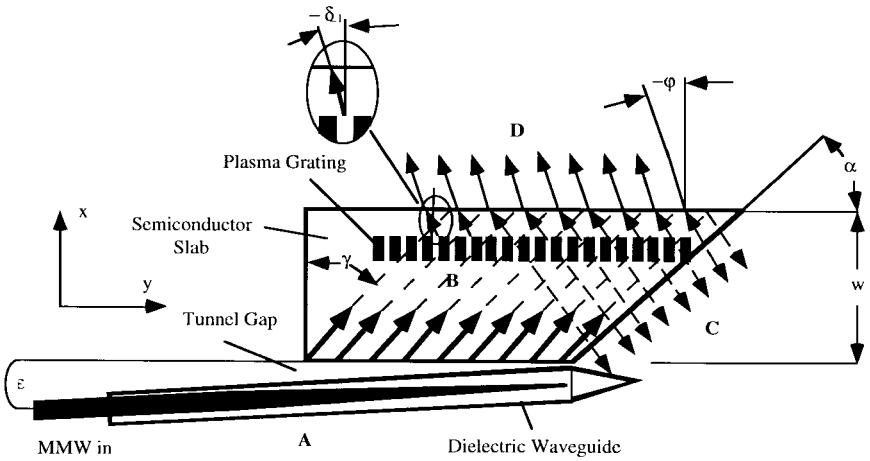


Fig. 2. PIPG antenna's ray geometry.

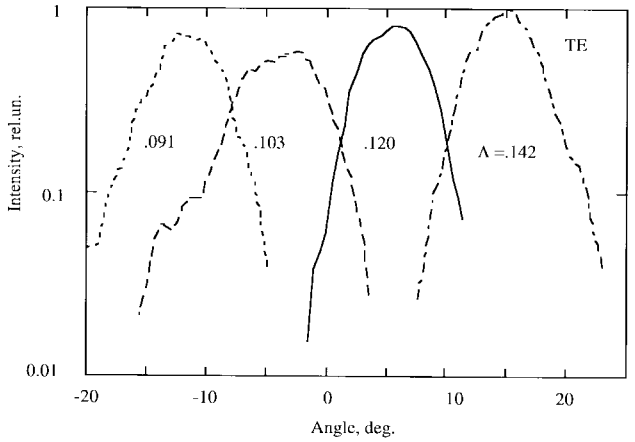


Fig. 3. Far-field antenna patterns for TE polarization.

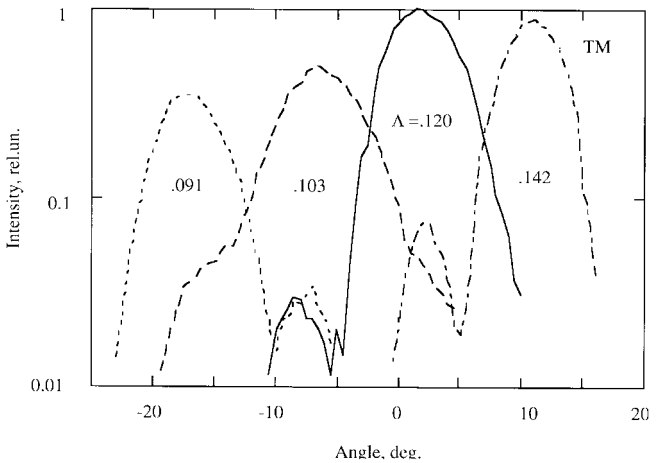


Fig. 4. Far-field antenna patterns for TM polarization.

the angle $\varepsilon$ as follows:

$$\gamma = \arcsin[(\beta_{\text{wg}} \cos\varepsilon)/\beta_{\text{sl}}]. \tag{1}$$

If the photo-induced grating is parallel to the lower edge of the slab, Beam **B** impinges upon the grating at the same angle $\gamma$. The grating diffraction orders will propagate in directions described by angles, $\delta_p$, defined by the equation

$$\beta_{\text{sl}} \sin\delta_p = \beta_{\text{sl}} \sin\gamma + p(2\pi/\Lambda) \tag{2}$$

where $p = \cdots -1, 0, +1, +2, \cdots$, is the diffraction order.

One can show that under the following conditions:

$$[\beta_{\text{sl}}(1+\sin\gamma)]^{-1} < \Lambda/2\pi < \{[\beta_{\text{sl}}(1-\sin\gamma)]^{-1} \cup 2[\beta_{\text{sl}}(1+\sin\gamma)]^{-1}\} \tag{3}$$

there exist only 0 and $-1$ diffraction orders ($p = 0, -1$).

When these beams impinge upon the upper edge of the semiconductor slab, which is parallel to the lower edge, they experience reflection and refraction. Now, if

$$\beta_{\text{wg}} \cos\varepsilon > k_0 \tag{4}$$

where $k_0 = 2\pi/\lambda$ is the propagation constant in free space (and $\lambda$ is the MMW wavelength in vacuum), then according to (1), the angle $\gamma$ is larger than the total internal reflection angle (TIR), $\text{TIR} = \arcsin(k_0/\beta_{\text{sl}})$. The important consequence of this is that the 0-order beam is totally reflected from the slab/air interface and does not contribute to the output beam. The remaining $-1$-order beam is partially reflected back (*not* shown in Fig. 2) and partially refracted. The refracted part provides the main contribution to the output beam (Beam **D**). This beam propagates in a direction corresponding to an angle $\varphi$ as follows:

$$\varphi = \arcsin[\beta_{\text{sl}} \sin(\delta_{-1})/k_0] \tag{5}$$

or, after substitution from (1) and (2)

$$\varphi = \arcsin[\beta_{\text{wg}} \cos(\varepsilon)/k_0 - \lambda/\Lambda]. \tag{6}$$

From (6), one can see that the angle $\varphi$ does not depend on the propagation constant in the semiconductor slab, $\beta_{\text{sl}}$. Moreover, if due to the small value of the angle $\varepsilon$, one assumes $\cos(\varepsilon) \cong 1$, then the angle $\varphi$ coincides with the angle of radiation from a dielectric rod loaded with a metal grating of the same period $\Lambda$ [8] as follows:

$$\varphi \cong \arcsin(\beta_{\text{wg}}/k_0 - \lambda/\Lambda). \tag{7}$$

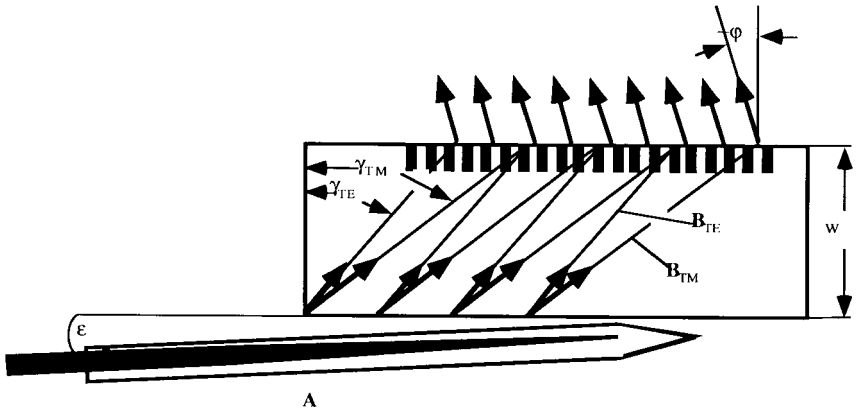


Fig. 5. Conversion of a linear polarized input beam into a circularly polarized output beam.

## III. Beam-Steering Experiment

From (6), one can see that the output beam angle can be controlled by varying the grating period $\Lambda$. In the experiment, this was accomplished by changing the grating pattern of the photo-masks.

A silicon 17.5-mil-thick slab cut from a float-zone ingot acts as a single-mode planar waveguide where both the $\mathrm{TE}_0$ or $\mathrm{TM}_0$ modes can propagate. The dielectric waveguide feeder was made from a circular quartz rod and was coupled to a MMW source or detector. The experiment was performed at the frequency of 90 GHz, the respective propagation constants were found to be $\beta_{\mathrm{TE}} = 51.3$ cm$^{-1}$ and $\beta_{\mathrm{TM}} = 26.7$ cm$^{-1}$. Obviously, the TIR condition for these two modes is different, which determined our choice of two different experimental geometries: for TE polarization $w = 1.5$ in, $\alpha = 40.5°$, and for TM polarization $w = 0.51$ in and $\alpha = 24°$ (see Fig. 2). The prismatic angle $\alpha$ provided close to normal incidence for the TIR Beam **C**. This geometry, along with the tapered edge of the waveguide, assured removal of the unwanted Beam **C** (0 order) and minimized its contribution to the output beam. The measurements were performed for two output polarizations of Beam **D**, which were identical to the input polarizations provided by the MMW source and were maintained in the respective antenna configurations.

The PIPG's were generated by illuminating the silicon planar waveguide through photo-masks with four different grating periods: $\Lambda = 0.091,\ 0.103,\ 0.120$, and $0.142$ in. The PIPG's were excited close to the upper edge of the slab. The periods of the PIPG's differed a little from that of the photo-masks because the photo-masks were slightly rotated (individually for each grating and each polarization) to obtain maximum efficiency. The source of illumination was a stroboscopic arc lamp. The lamp produced pulses with a duration of 2 $\mu$s, repetition rate of 100 Hz, and energy density of $0.5 \cdot 10^{-4}$ J/cm$^2$ per pulse at the silicon surface.

The radiating aperture of the antenna in the scanning plane is defined by the slab length, the grating length, and by the length of the tunnel coupling between the quartz rod and the slab. In the scanning direction, the aperture size was approximately 1.2 in. To form the MMW beam in the perpendicular direction, a cylindrical lens (with an aperture of 1 in) was used.

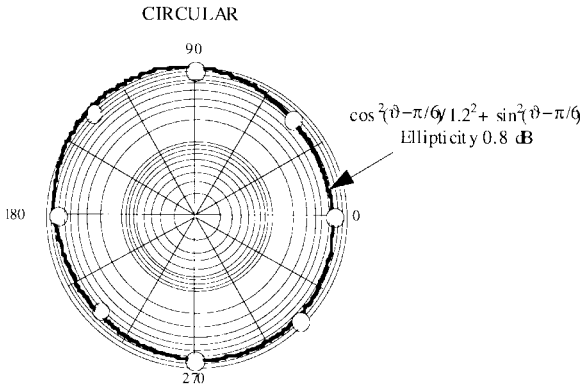


Fig. 6. Experimental diagram of the circularly polarized output beam.

The antenna was tested in both the transmitting and receiving modes. In both modes, the antenna performance was similar. The far-field antenna patterns for two orthogonal polarizations are shown in Figs. 3 and 4, respectively. The directions of the output beams were in good agreement with the predictions based on (6), assuming that $\beta_{\mathrm{wg}}$ is close to the theoretical value, of 20.2 cm$^{-1}$. Any small differences in angular positions between the two polarizations can be explained by different alignment of the photo-masks required to achieve maximum antenna efficiency. To estimate the performance of our antenna, we replaced our antenna with a standard gain horn with a claimed gain of 25 dB (made by Aeroware Inc., MA). We used exactly the same measurement setups for both antennas. In both the transmitting and the receiving modes, our antenna produced signals at a level of $-8$ dB, comparable to the reference horn.

## IV. Circular Polarization

As we already noted, for any given grating period $\Lambda$, the angle $\varphi$ of the output beam should not depend on the propagation constant of the planar waveguide, and thus remains the same for both the $\mathrm{TE}_0$ and the $\mathrm{TM}_0$ modes. If one excites both these modes, the output beam will be a superposition of the respective polarizations. By properly choosing the phase delay between the two linear polarizations, we can obtain a circularly polarized output beam even though the input MMW source is linearly polarized. The required phase delay can be

achieved by utilizing the difference in propagation constants and in the in-slab propagation angles $\gamma$ for the two orthogonal polarizations. Fig. 5 illustrates the concept. Let the original Beam $\mathbf{A}$ be linearly polarized in a direction forming an angle, $\rho \cong 45°$, with the slab plane (the plane of the drawing). The input Beam $\mathbf{A}$ excites two orthogonal modes propagating in the planar slab waveguide. These two modes have distinct propagation constants $\beta_{\mathrm{TE}}$ and $\beta_{\mathrm{TM}}$ and these propagate at different angles ($\gamma_{\mathrm{TE}}$ and $\gamma_{\mathrm{TM}}$) in the slab. In general, they arrive at the emitting surface of the slab (antenna aperture) at different phases. By properly selecting the slab width $w$ we can make the phase difference between the two combining beams at the antenna aperture to be $\pi/2$. If the amplitudes of the $\mathrm{TE}_0$ and $\mathrm{TM}_0$ propagating modes are equal, then the output beam will be circularly polarized.

To prove this concept, an experiment was performed using a planar slab waveguide with a width $w = 0.756$ in. A linearly polarized MMW source was set up to feed a circular dielectric waveguide at a polarization angle, $\rho \cong 45°$. The slab was illuminated through a photo-mask with $\Lambda = 0.120$ in. A circular horn antenna with an attached detector was mounted on a rotating base with an axis coinciding with the axis of the horn. It was installed in the far-field region in the direction of the antenna main lobe. We found that the output beam was elliptically polarized. It was then tuned into circular polarization by adjusting the angle $\rho$. The remaining ellipticity was less than 0.8 dB, as seen in Fig. 6. When the input MMW radiation was polarized in the plane of the slab $(\rho = 0)$ or perpendicular to that plane $(\rho = 9°)$, the intensity of the output beams obeyed the cosine square law, confirming linear polarization.

## V. Summary

An optically controlled antenna based on a new architecture has been proposed and experimentally demonstrated. A semiconductor (silicon) plate is the photosensitive medium which provides the antenna with the beam-steering (and eventually beam-forming) capability through a PIPG. In our preliminary experiments in creating a grating pattern, we used a set of photo-masks. We are currently updating the antenna design by utilizing optical fibers fed by an array of switchable LED's. We have already achieved an antenna performance comparable with that obtained with the fixed masks illumination. Fiber-optics illumination allows one to implement dynamic control and flexibility expected of electronically scanning antennas, but at a dramatically lower cost. Another advantage of the proposed architecture is the antenna's ability to operate at various polarizations: linear (vertical or horizontal), as well as circular (elliptical). In the present architecture, the described antenna has a limited bandwidth as it is characterized by a 0.6°/GHz dispersion factor.

## Acknowledgment

The authors would like to thank R. Gajewski for his insight and technical discussions.

## References

[1] C. H. Lee, P. S. Mark, and A. P. DeFonzo, "Optical control of millimeter-wave propagation in dielectric waveguides," *IEEE J. Quantum Electron.*, vol. QE-16, pp. 277–288, 1980.

[2] M. Matsumoto, M. Tsutsumi, and N. Kumagai, "Radiation of millimeter waves from a leaky dielectric waveguide with a light-induced grating layer," *IEEE Trans. Microwave Theory Tech.*, vol. MTT-35, pp. 1033–1052, 1987.

[3] A. Rosen, P. J. Stabile, P. Herczfeld, A. Daryoush, and J. K. Butler, "Optically controlled IMPATT diodes and subsystems," in *Proc. 1989 SBMO Int. Microwave Symp.*, vol. II, 1989, pp. 589–594.

[4] V. A. Manasson, L. S. Sadovnik, P. I. Shnitser, and V. Litvinov, "Guided wave antenna induced by light," presented at the *Proc. 1994 Antenna Applicat. Symp.*, Allerton Park, IL, 1994.

[5] V. A. Manasson, L. S. Sadovnik, A. Moussessian, and D. B. Rutledge, "Millimeter-wave diffraction by a photo-induced plasma grating," *IEEE Trans. Microwave Theory Tech.*, vol. 43, pp. 2288–2290, Sept. 1995.

[6] A. Alphones and M. Tsutsumi, "Leaky wave radiation from a periodically photoexcited semiconductor slab waveguide," *IEEE Trans. Microwave Theory Tech.*, vol. 43, pp. 2435–2441, Sept. 1995.

[7] V. A. Manasson, L. S. Sadovnik, P. I. Shnitser, and R. Mino, "Millimeter-wave optically scanning antenna based on photoinduced plasma grating," *Opt. Eng.*, vol. 35, no. 2, pp. 357–361, 1996.

[8] F. K. Schwering and A. A. Oliner, "Millimeter-wave antennas," in *Antenna Handbook: Theory Applications and Design*, Y. T. Lo and S. W. Lee, Eds. New York: Van Nostrand, 1988, ch. 17, pp. 1–150.

**V. A. Manasson** (A'96), photograph and biography not available at the time of publication.

**L. S. Sadovnik** (A'95), photograph and biography not available at the time of publication.

**V. A. Yepishin** (A'96), photograph and biography not available at the time of publication.

**D. Marker**, photograph and biography not available at the time of publication.